Computer Methods and Recent Advances in Geomechanics – Oka, Murakami, Uzuoka & Kimoto (Eds.)
© 2015 Taylor & Francis Group, London, ISBN 978-1-138-00148-0

Evaluation of dynamic behavior of culverts and embankments through centrifuge model tests and a numerical analysis

Y. Sawamura, K. Kishida & M. Kimura
Kyoto University, Kyoto, Japan

ABSTRACT: In the design of culverts in Japan, the effects of earthquakes are not usually considered in the design of conventional culverts. This is because culverts are thought to follow the deformation of the surrounding soil. Due not only to the increase in construction opportunities involving high embankments, but also to the development of new forms of culverts, such as precast arch culverts, which contain hinge structures, it is becoming more and more important to clarify the seismic performance of those culvert embankments. In this study, dynamic centrifuge modeling tests and a numerical analysis were carried out to clarify both the mechanical influence of the structural shape and the height condition of the embankment. From the results, it was found that the effect of the embankment condition on the increments in bending moments varies greatly depending on the structural shape of each culvert.

1 INTRODUCTION

In the design of culverts in Japan, conventional culverts have been built over the past many years by applying methods which do not consider an aseismic design. This is because of the presupposition that culverts act in accordance with the surrounding soil or banking in an integrated manner and that the seismic force acting on the culverts is small for the range of conventional culverts. In recent years, however, construction opportunities for culverts which are outside the range of conventional culverts, such as large sections, high-fill conditions and precast culverts, which include hinges in the main body, are increasing. Therefore, the evaluation of the seismic capacity of culverts has become an important issue.

Regarding the seismic stability of box culverts, there has been much advanced research intended for underground structures. Matsui et al. (2004) conducted large shake table tests and a subsequent numerical analysis correlation to develop and validate a suitable nonlinear FEM model for the seismic performance evaluation of underground RC box culverts. Nam et al. (2006) proposed the elasto-plastic interface model for the seismic analysis of underground RC structures, and simulated the failure mechanisms of underground box culverts under seismic action.

On the other hand, few studies have been done on the hinge type of precast arch culverts. Wood et al. (2000) conducted a site-specific finite element analysis to develop an earthquake design procedure for the three-hinge precast arch culvert method. They concluded that the bending moments in the arch, due to horizontal earthquake loading, can be significant in relation to the gravity load action. Hinged precast culverts have a reasonable structural shape or an intermediate structural shape between that of rigid culverts and flexible culverts, but are not covered by the Japanese standard specifications for culvert construction. Thus, each construction method, such as the two-hinge precast arch culvert method and the three-hinge precast arch culvert method, is applied to examine its earthquake resistance according to its own rules. From now on, a comprehensive design method, that can reflect the characteristics of each structural shape of culvert and includes earthquake resistance, should be created.

In this study, dynamic centrifugal model tests and a numerical analysis that focus on both the mechanical influence of the structural shape and the height condition of the embankment were conducted to clarify the behavior of culvert embankments.

2 EXPERIMENT AND ANALYSIS CONDITION

2.1 *Centrifuge model tests*

2.1.1 *Experimental set-up*

Centrifuge model tests were performed under a gravitational acceleration of 50 G. A soil chamber, 450 mm long, 300 mm deep and 150 mm wide, with a transparent front window, was used for the tests. In this study, two types of embankment conditions and three types of culvert models were used. The experimental models represented a fill of 5.0 m (low embankment condition) and 7.5 m (high embankment condition) to be constructed on a sandy ground with a thickness of 5.0 m. The structural shape of the culverts varied, namely, (a) Box culvert model, (b) Rigid arch culvert model, whose shoulders are rigidly connected,

Table 1. Examination cases.

Case	Type of culvert	Height of embankment [m]	Overburden [m]
Case-0_L	No culvert	5.0	–
Case-1_L	Box	5.0	0.5
Case-2_L	Rigid arch	5.0	0.7
Case-3_L	2-hinge arch	5.0	0.7
Case-0_H	No culvert	7.5	–
Case-1_H	Box	7.5	3.0
Case-2_H	Rigid arch	7.5	3.2
Case-3_H	2-hinge arch	7.5	3.2

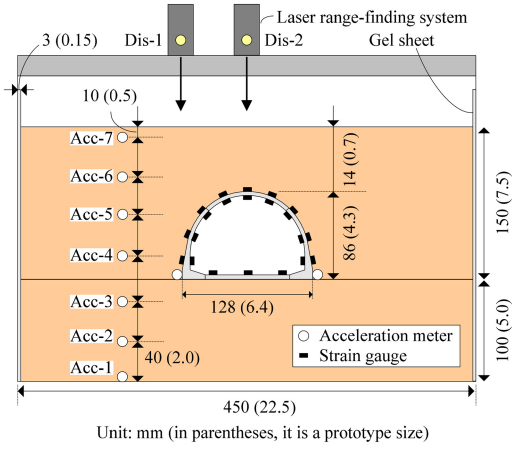

Unit: mm (in parentheses, it is a prototype size)

Figure 1. Diagrammatic illustration (High embankment condition).

and (c) 2-hinge arch culvert model, which contains a hinge structure in both shoulders. The results from these three patterns were compared to a fill-only case without a culvert. Table 1 shows the experiment cases. Figure 1 shows the set-up of the culvert model and the arrangement of the sensors and strain gauges.

2.1.2 *Culvert models*

Figure 2 and Photo 1 show the dimensions of the culvert models and a photograph of each model, respectively. The rigid arch model and the 2-hinge arch model had the same section except for the hinges in the shoulder parts. Moreover, the box model and the arch model were designed so that the outer width of the two models would be equivalent. The culvert models used in the experiment were made from mortar. Table 2 shows the material constants for the culvert models.

2.1.3 *Model ground and input wave*

Both the foundation ground and the filling were made from dry Toyoura sand using a sand hopper. The falling height of the sand was adjusted in such a way that a relative density of 85% was achieved. Table 3 shows the properties of Toyoura sand.

Gel sheets, 3 mm in thickness, were inserted as cushioning between the soil and the soil chamber in the

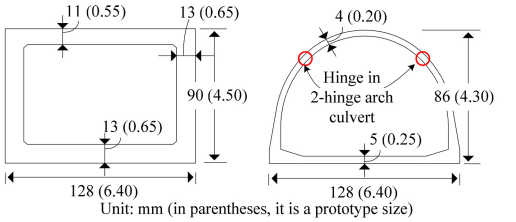

Unit: mm (in parentheses, it is a prototype size)

(a) Box culvert (b) Rigid and 2-hinge arch culvert

Figure 2. Dimensions of culvert models.

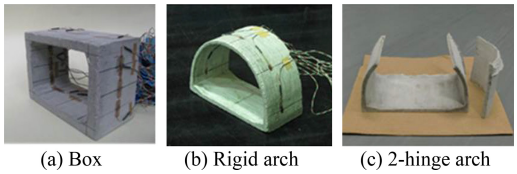

(a) Box (b) Rigid arch (c) 2-hinge arch

Photo 1. Culvert models using centrifuge model tests.

Table 2. Material constants of culvert models.

Property	Culvert
Young's modulus E [kN/m^2]	2.07×10^7
Unit weight γ [kN/m^3]	19.35
Compressive strength f_c [N/m^2]	4.92×10^4
Bending strength f_b [kN/m^2]	1.17×10^4
Tensile strength f_t [kN/m^2]	5.76×10^3
Poisson's ratio ν	0.18

Table 3. Properties of Toyoura sand.

Property	Toyoura sand
Specific gravity G_s	2.64
Unit weight γ [kN/m^3]	15.8
Average diameter D_{50} [mm]	0.20
Maximum void ratio e_{max}	0.975
Minimum void ratio e_{min}	0.585
Void ratio e	0.642

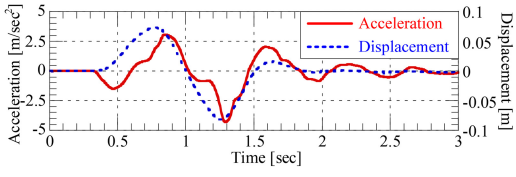

Figure 3. Time history of acceleration and displacement measured at shaking table in Case-0_L.

direction of the shaking in order to reduce the reflected wave from the boundary of the soil chamber.

The one sine wave of the prototype, 1Hz, was inputted by controlling the displacement of the vibration table. Figure 3 shows the time history of the acceleration and the displacement measured at the shaking table in Case-0.

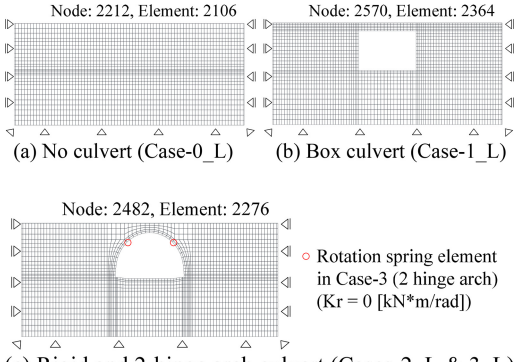

Figure 4. Analytical mesh and boundary conditions (Low embankment condition).

2.2 *Numerical analysis*

2.2.1 *Numerical code and FEM mesh*

In this study, a 2-D elasto-plasticity FEM analysis was performed using a program called 'DBLEAVES' (Ye et al., 2007). Since a rigid soil chamber was used in the experiment, the analytical domain was made to be the same size as the soil chamber with both sides horizontally restrained. The analytical mesh and the boundary conditions are shown in Figure 4.

The input ground motions used in this analysis are from the time history of the acceleration measured by Case-0 of the experiment shown in Figure 3. In the dynamic analysis, viscous damping is adopted, the direct integration method of Newmark-β ($\beta = 1/4$, $\gamma = 1/2$) is used and the time interval of the calculation is 0.0005 seconds.

2.2.2 *Modeling of ground and culverts*

The constitutive model for Toyoura sand is the subloading t_{ij} model (Nakai and Hinokio, 2004). This model was proposed based on the concept of SMP (Spatially Mobilized Plane), in which the influence of the intermediate principal stress can be properly evaluated. Furthermore, this model can describe the dependence of the direction of the plastic flow on the stress paths and the dependence of the density and the confining pressure on the deformation and strength of the soil. The parameters of Toyoura sand are given in Table 4. As a rigid soil chamber was used in the experiment, there is a high degree of potential for the damping ratio of the soil to be higher than in the in-situ construction. Therefore, a pre- analysis, in which the damping coefficient of the ground was a changing parameter ($h = 5$, 10, 20, 30, 40 and 50 %), was conducted preliminarily, and then the ratio was determined to be 30%.

While modeling the structure, the nonlinearity of the concrete was also considered. For culvert concrete, the nonlinear moment-curvature relation was simulated using the AFD (Axial Force Dependent) model (Zhang and Kimura, 2002). The axial-force dependency, according to the variable axial force of the structure, can be considered by using this model.

Table 4. Parameters of Toyoura sand.

Property	Culvert
$R_{CS} = (\sigma_1/\sigma_3)_{CS(comp.)}$	3.2
Compression index λ	0.07
Swelling index κ	0.0045
$N = e_{NC}$ *at* $p = 98$ kPa & $q = 0$ kPa	1.1
β	2.0
a	60
Poisson's ratio ν	0.333

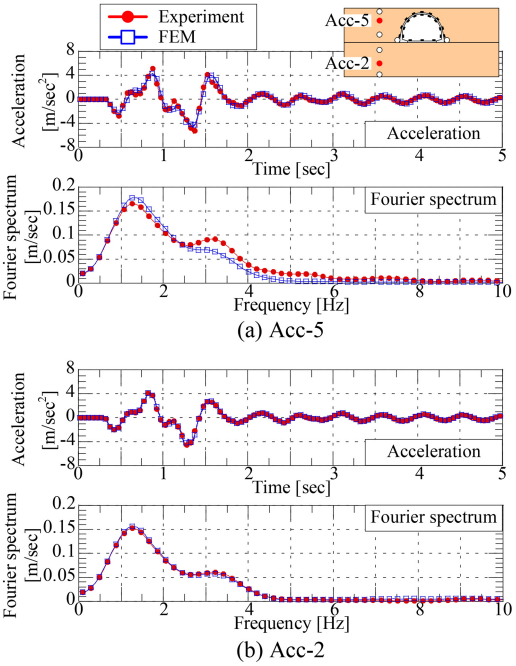

Figure 5. Time history of acceleration and Fourier spectrum of Acc-2 and Acc-5 for Case-3 (Low embankment condition).

Moreover, the joint element was arranged on the boundary between the culverts and the ground to represent the influence of friction. The parameters of the joint element were defined from box shear tests between Toyoura sand and the concrete element. And the damping coefficient of the culverts was assumed as 2%.

3 ANALYSIS RESULTS

3.1 *Comparison of experiments*

In this chapter, the results of the experiment and the numerical analysis under a low embankment condition are compared, and the applicability of the numerical analytical approach is evaluated.

First, Figure 5 shows the time history of the acceleration and the Fourier spectrum of Acc-2 and Acc-5 for Case-3 which contains a 2-hinge arch culvert in the banking. From this figure, it can be seen that the

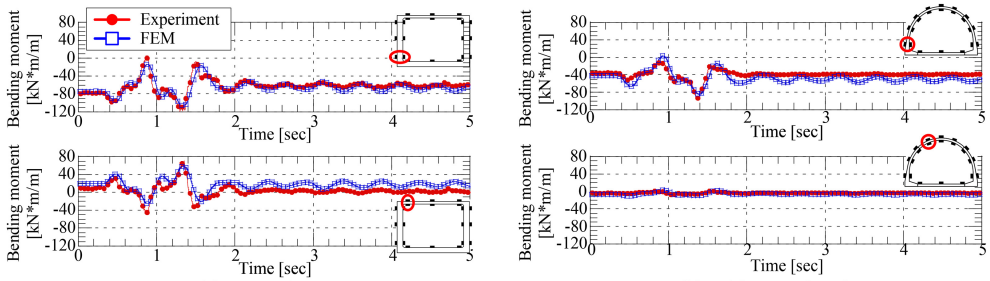

Figure 6. Time history of bending moment in box culvert (Case-1) and 2-hinge arch culvert (Case-3) (Low embankment condition).

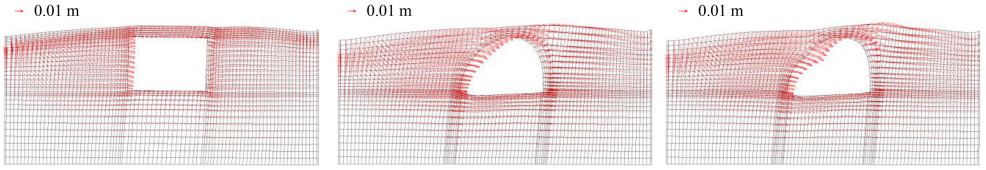

Figure 7. Deformation diagram (output of displacement: 50 times) when maximum bending moment is generated at left foot (Low embankment condition).

response acceleration spectrum and its Fourier spectrum obtained from the analysis precisely replicate the experiment in Acc-2, and that the analytical value can reproduce the experimental value to some extent also in Acc-5. When the difference between the experimental and the analytical values in Acc-5 is looked at in detail, the acceleration obtained from the analysis tends to become small in the vicinity of the maximum and the minimum values compared with the acceleration obtained from the experiment. In the Fourier spectrum, the high-frequency component near 3.5 Hz, considered to be the cause of such a phenomenon, is small compared to the experimental value. However, as a whole, the analytical value reproduces the experimental value accurately. Moreover, the numerical analysis was able to reproduce the experiment with the same accuracy as Case-3 in other cases too.

The time history of the bending moments in each position in the box culvert (Case-1) and the 2-hinge arch culvert (Case-3) is shown in Figure 6. A positive bending moment is defined for the case in which tension is generated inside the culverts. It can be seen that the analytical results reproduce the experimental results comparatively well, although the behavior after two seconds becomes a little large.

Based on the above results, the experimental study could be simulated accordingly in the present study by using a constitutive model for the ground and the culverts.

3.2 *Behavior of culverts under a low embankment condition*

In addition to the bending moments, some indexes, such as the deformation of culverts and the earth pressure distribution acting on culverts, which are difficult to measure in experiments, are discussed.

Figure 7 shows the deformation diagram (output of displacement: 50 times) when the maximum bending moment is generated at the left foot. For the box culvert, the ground over the culvert is displaced with uniformity. Furthermore, compared with the deformation of the surrounding soil, the shear deformation of the culvert is small. On the other hand, for the rigid arch culvert, the culvert deformed in such a way that the ground rose from the right shoulder to the top. Moreover, as a result of the culvert's shear deformation, the left side of the bottom deformed outside. In the 2-hinge arch culvert, since the shoulder is a hinge structure, the left side shoulder is displaced on the inside and the deformation becomes still larger than that of the rigid arch culvert.

Figure 8 shows the distributions of bending moments, axial force and earth pressure of the normal direction which act on the boundary portions of the ground and culverts in each case. In this figure, the line with the circle means the initial state, while the line with the square shows when the maximum bending moment is generated at the left foot.

Taking a look at the distribution of the distribution of earth pressure in the box culvert, although the box culvert has a cave, there is no difference in earth pressure acting on the bottom plate between the center and the end of the culvert at the initial state. This is because the whole rigidity of the box culvert is high; the installation pressure shows the same tendency as the rigid body foundation. When the maximum bending moment is generated at the left foot, a large bending moment is generated at the corner of the intersection of the left-hand side wall bottom and the right-hand

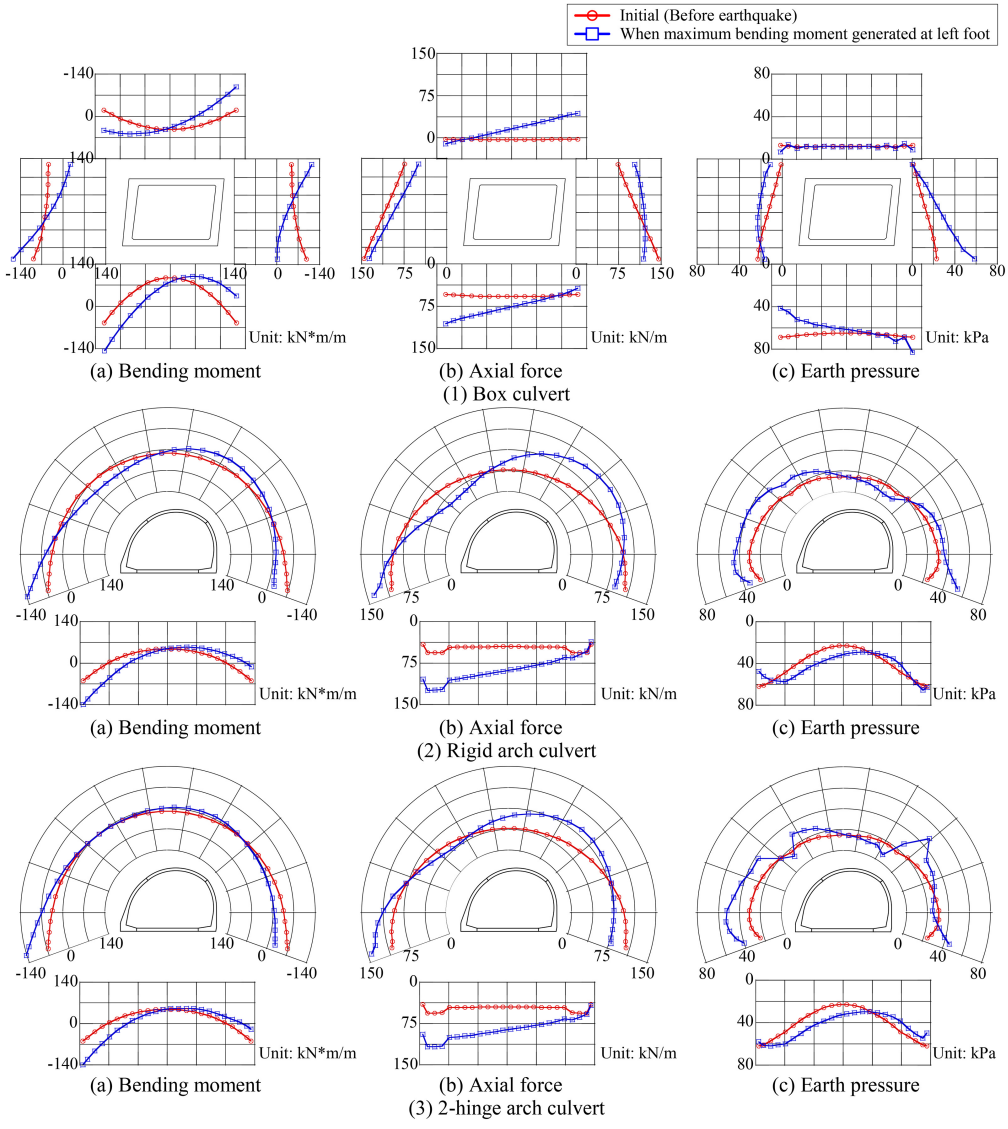

Figure 8. Distributions of bending moment, axial force and earth pressure of normal direction which act on boundary portions of ground and arch culvert (Low embankment condition).

side wall top. At that time, the axial force near the left foot becomes smaller than that at the initial state. The characteristic phenomenon is the earth pressure at the bottom. In the box culvert, the maximum bending moment is generated at the left foot, while larger earth pressure than at the initial state occurs at the right bottom, but the earth pressure is smaller than that at the initial state at the left bottom. This phenomenon suggests that the rigid body rotation mode excels in a box culvert since the whole rigidity is high.

Next, let's take a look at the rigid arch culvert. As compared with the box culvert, the earth pressure in the center of the culvert bottom at the initial state is small in the rigid arch culvert. This is due to the fact that the sectional force becomes large at both feet since the arch culvert may have a support mechanism through the axial force, and the center of the bottom transforms into an inner side as a result. When the maximum bending moment is generated at the left foot during an earthquake, a negative bending moment occurs in the left foot and the right shoulder, and a positive bending moment occurs in the left shoulder. This shows that not only the foot, but also the shoulder is subjected to the seismic force in a rigid arch culvert. Moreover, the axial force increased in the left foot and the right shoulder with a negative bending moment, and the axial force decreased in the left shoulder with a positive bending moment. The distribution of earth pressure differs for the rigid arch culvert and the box culvert. Although the rigid body rotation mode excels and earth

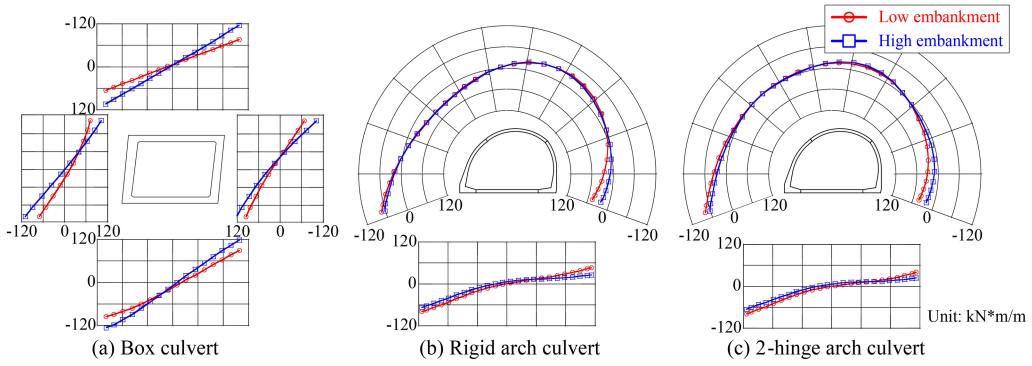

Figure 9. Distributions of increments in bending moment under low and high embankment conditions.

pressure at the left end of the bottom is smaller than at the initial state in the box culvert, the earth pressure at the left end of the bottom increased in the rigid arch culvert. The reason the earth pressure increased at the left side of the bottom is that the corner of the intersection of the bottom and the side wall has been bent, and the bottom plate is displaced greatly when the arch becomes shear and deforms greatly. Therefore, when the maximum bending moment is generated in the left foot, the earth pressure becomes large at the left end of the bottom.

Finally, the results of the 2-hinge arch culvert are discussed. In the 2-hinge arch culvert, the bending moment that occurs in the shoulder hardly changing from zero. Since the bending moment is not generated at the shoulder during earthquakes, the burden rate of the foot becomes large. From this, it can be said that only foot is subjected to the seismic force in a 2-hinge arch culvert. Although the earth pressure becomes a discontinuous distribution at the shoulder (hinge part) in the 2-hinge culvert, on the whole, the same tendency as the rigid arch culvert is shown. Moreover, since the shear modification became large in the 2-hinge arch culvert, the earth pressure becomes larger than for the rigid arch culvert.

3.3 *Influence of banking height*

Figure 9 shows the distribution of increments in bending moment. In this figure, the line with the circle means the low embankment condition, while the line with the square means the high embankment condition. In this paper, the increment in bending moment is defined as the difference between the initial and the maximum bending moments.

In the box culvert, the increment in bending moment increases in proportion to the banking height, and the tendency is remarkable at the corner of the intersection. On the other hand, in the rigid arch culvert and the 2-hinge arch culvert, the increment in bending moment stays almost constant regardless of the banking height. That is, while the banking condition affects the initial section force and the seismic modification of the culvert in box culverts, the banking condition affects only the sectional force of the initial state in the arch culverts. Therefore, it can be concluded that the increments in sectional force in arch culverts do not change regardless of the banking height; the arch culverts are structures that are hard to subject to the influence of the banking height during earthquakes.

4 CONCLUSIONS

In this study, dynamic centrifugal model tests and a numerical analysis that focused on both the mechanical influence of the structural shape and the height condition of the embankment were conducted. The following conclusions can be drawn from the results of this study:

(1) The experimental study was simulated accurately in the present study by using a constitutive model for the ground and the arch culverts.
(2) The effect of the embankment conditions on increments in bending moment were seen to vary greatly depending on the structural shape of the culvert.

REFERENCES

Matsui, J., Ohtomo, K. & Kanaya, K. 2004. Development and validation of nonlinear dynamic analysis in seismic performance verification of underground RC structures, *Journal of Advanced Concrete Technology* 2(1): 25–35.

Nakai, T. & Hinokio, M. 2004. A simple elastoplastic model for normally and over consolidated soils with unified mate-rial parameters. *Soils and Foundations* 44(2): 53–70.

Nam, S. H., Song, H. W., Byun, K. J. & Maekawa, K. 2006. Seismic analysis of underground reinforced concrete structures considering elasto-plastic interface element with thickness, *Engineering Structures* 28: 1122–1131.

Wood, J. H. & Jenkins, D. A. 2000. Seismic analysis of buried arch structures, *Proc. of the 12th World Conference of Earthquake Engineering*, No. 0768.

Ye, B., Ye, G. L., Zhang, F. & Yashima, A. 2007. Experiment and numerical simulation of repeated liquefaction – consolidation of sand, *Soils and Foundations* 47(3): 547–558.

Zhang, F. & Kimura, M. 2002. Numerical prediction of the dynamic behaviours of an RC group-pile foundation. *Soils and Foundations* 42(3): 72–92.